Histol Histopathol (2002) 17: 427-436

http://www.hh.um.es

Histology and Histopathology

Cellular and Molecular Biology

Disorganization of honey-comb immunoreactive pattern of desmin and plectin in rat atrophic soleus muscle fiber induced by hindlimb suspension

S. Nara[1,3], K. Hachisuka[1], H. Furukawa[2], Y. Doi[3], H. Kudo[3] and S. Fujimoto[3]

Departments of [1]Rehabilitation Medicine and [3]Anatomy, School of Medicine, [2]Department of Clinical Pathology, School of Health Sciences, University of Occupational and Environmental Health, Kitakyushu, Japan

Summary. Immunoreactivity for desmin, plectin and α-actinin was investigated in rat atrophic soleus muscle fibers induced by hindlimb suspension between 1 and 4 weeks (hindlimb suspension group, HSG), and compared with that of the control group (CG). Some of the HSG for 4 weeks were allowed unrestricted cage activity for 2 weeks as the recovery group (RG). In the cross-sectioned muscle fibers of the CG, desmin and plectin showed honey-comb immunoreactive patterns extending throughout the sarcoplasm. Superimposed images by double immunofluorescence labeling showed overlapping of both immunoreactivities. In the longitudinally sectioned profiles, superimposed images of α-actinin and desmin were overlapped at the level of Z-discs. The focal disorganization of the above honey-comb immunoreactive patterns, followed by the reduction of the cross-sectional area (CSA) of atrophic soleus muscle fibers and the appearance of Z-streaming, uniquely arose in the HSG from the first week and extended throughout the sarcoplasm in proportion to the suspension period. Such honey-comb patterns of both desmin and plectin were already restored in the RG at 2 weeks, followed by the disappearance of Z-streaming, prior to the recovery of the CSA. These findings indicate that the disorganization of topological and structural relationships of desmin and plectin with Z-discs surrounding individual myofibrils is primarily evoked, which leads to Z-streaming of atrophic soleus muscle fibers, and that the restoration of the muscle activity results in an early arrangement recovery of desmin and plectin around myofibrils.

Key words: Alpha actinin, Desmin, Hindlimb suspension, Immunocytochemistry, Muscle atrophy, Plectin

Offprint requests to: Soichiro Nara, M.D., Department of Anatomy, University of Occupational and Environmental Health, School of Medicine, Kitakyushu 807-8555, Japan. Fax: +81-93-692-0121. e-mail: so-nara@med.uoeh-u.ac.jp

Introduction

In addition to the induction by neural and endocrine dysfunction (Russman et al., 1983; Price et al., 1987; Zurcher et al., 1989; van Balkom et al., 1994), malnutrition (Hansen-Smith et al., 1979; Brooks, 1995) and microgravity (Booth and Gollnick, 1983; Fitts et al., 2000), muscle atrophy is induced by cast-fixation for orthopedic treatment, and the pathogenesis of muscle atrophy induced by various causes has been one of the important research fields in rehabilitation medicine. Up to now, morphological and physiological alterations of experimentally-induced skeletal muscle atrophy by a variety of methods have been investigated by many researchers (Valtat, 1877; Lippmann and Selig, 1928; Thompsen and Luco, 1944; Booth, 1977; Goldspink, 1977; Witzmann et al., 1982).

Since the classic description of a remarkable decrease in wet weight of immobilized skeletal muscles of dogs and guinea pigs by Valtat (1877), histological findings, concerning the reduction in diameter of atrophic muscle fibers (Thompsen and Luco, 1944), the difference in degree of atrophy among different fiber types (Desplanches et al., 1987; Hauschka et al., 1988), and the recovery process of atrophic muscle activity (Fitts and Brimmer, 1985; Thomason et al., 1987; Mozdziak et al., 2000) have been discussed in reference to physiological data on the decline of atrophic muscle activities. At the electron microscopic level, waving and distortion of Z-discs, generally called Z-streaming (Cooper, 1972), and the disorganization of bundles of myofilaments (Tomanek and Lund, 1974) have also been related to a loss or decline of atrophic muscle activities.

Since Ishikawa et al. (1968) first described the crucial roles of intermediate filaments (IFs) in the maintenance of structure and function as cytoskeleton of skeletal muscle fibers, ultrastructural, immunocyto-chemical and immunological analyses on topological relationships and roles of IFs have been made using animals congenitally devoid of IFs (Li et al., 1996; Milner et al., 1996; Andrä et al., 1997). Desmin belongs

to IFs in all kinds of muscle fibers (Bennett et al., 1979; Lazarides, 1980), and plectin is an IF-associated protein (Foisner and Wiche, 1991). In skeletal muscle fibers, plectin is localized at the level of Z-discs as well as beneath the sarcolemma (Wiche et al., 1983; Gache et al., 1996; Andrä et al., 1997; Schröder et al., 1997). Recently, Hijikata et al. (1999), after combining electron microscopy with immunocytochemistry of rat diaphragma, proposed topological and structural relationships of desmin and plectin with Z-discs manifested by immunoreactivity for α-actinin, which play the crucial roles in effective force generation during muscle contraction and relaxation. Using immunoelectron microscopy, Schröder et al. (1999) revealed that plectin exists along the cytoplasmic face of the sarcolemma at regularly-spaced intervals as well as in filamentous bridges between Z-discs of the peripheral myofibrils and sarcolemma, forming the intermyofibrillar scaffold in human skeletal muscle fibers.

Up to now, immunoreactivity for desmin and plectin in atrophic muscle fibers hardly been surveyed (Schröder et al., 1997). Thus, we do not know whether immunoreactivity for desmin and plectin is altered in atrophic muscle fibers, and, if this is correct, whether such changes represent the disorganization of topological and structural relationships of desmin and plectin with Z-discs, which leads to Z-streaming. On these grounds, the present study was designed to investigate immunoreactivity for desmin and plectin and that for α-actinin on rat atrophic soleus muscles induced by hindlimb suspension. In addition, the present study includes the restoration in arrangement of desmin and plectin in the atrophic muscles that allow unrestricted cage activity.

Materials and methods

Animals

Male Wistar rats aged 11 weeks were acclimated for one week under the same feeding and water supply conditions. We followed the Guiding Principles for the Care and Use of Animals as set up by the University of Occupational and Environmental Health in accordance with principles of the Declaration of Helsinki (1964, revised in 1975 and 1983). Animals weighing 380-400 g were randomly assigned to the hindlimb suspension group (HSG), the recovery group (RG) or the control group (CG). Since hindlimb suspension of animals was performed under anesthesia with an intraperitoneal injection of diethyl ether and pentobarbital sodium (50 mg/kg), animals which were provided for the other groups were also anesthetized with the same dose and in the same manner to maintain equal acclimatized conditions.

For the HSG, hindlimbs were suspended for 1 (n=6), 2 (n=7) and 4 (n=19) weeks according to the tail-casting technique by Fitts et al. (1986). Some of the HSG for 4 weeks (n=12) were used for the RG, and were allowed unrestricted cage activity for 1 (n=6) and 2 (n=6) weeks after being removed from hindlimb suspension for 4 weeks. The CG was kept in unrestricted cages for 1 (n=6), 2 (n=6), 4 (n=6), 5 (n=4) and 6 (n=5) weeks. The HSG and RG were fed ad libitum, and the CG was pair-fed with the HSG and RG in order to maintain equal nutritious conditions. Cages for all groups were maintained at 22 °C and 50% humidity under a 12 hr light and dark cycle.

Assay of blood serum

Blood samples from all groups were collected from the left ventricle and centrifuged for 10 min at 2,000 g to obtain the blood serum, which was stored at nearly -40°C until use for the following assays: total protein according to the Biuret method using Total Protein-HR II (Wako, Osaka, Japan); albumin according to the BCG method using Albumin-HR II (Wako, Osaka, Japan); and total cholesterol according to the HDAOS method using L-type Wako CHO·H (Wako, Osaka, Japan). All values are shown in Table 1.

Electron microscopy

Isolated soleus muscles from all groups were fixed in a mixture of 2% paraformaldehyde (PFA) and 2.5% glutaraldehyde in 0.1M phosphate buffer (pH 7.2: PB) for 16 hr at 4 °C, postfixed in a solution of 1% osmium tetroxide in the buffer for 2 hr at 4 °C, dehydrated in graded concentrations of ethanol, and embedded in epoxy resin. Ultrathin sections were made on an ultramicrotome (MT-X, AZ, USA), stained with uranyl acetate and lead citrate, and examined in a JEM 1200 EX electron microscope.

Immunocytochemistry

Isolated soleus muscles from all groups were attached to cork boards with tragacanth gum, and then immersed in isopentane, which was chilled by liquid nitrogen at nearly -150 °C. Cryopreserved-frozen muscles at nearly -80 °C were transversely or longitudinally cut into approximately 10 µm-thick serial sections using a cryostat (Microm, Walldorf, Germany).

Sections, which were mounted on glass slides (MAS coated Superfrost, Matsunami, Osaka, Japan), were air-dried, incubated with 10% normal goat serum for 20 min at room temperature, and immunoreacted with the following monoclonal antibodies (mAb) for 18 hr at 4 °C: mouse anti-desmin mAb (clone DE-V-10, Sigma Chemical Co., St. Louis, MO) at a dilution of 1:20 in PBS; mouse anti-plectin mAb (clone 7A8; Sigma Chemical Co., St. Louis, MO) at a dilution of 1:100 in PBS; mouse anti-α-actinin mAb (clone EA-53, Sigma Chemical Co., St. Louis, MO) at a dilution of 1:400 in PBS; or mouse anti-ß dystroglycan mAb (clone 43DAG1/8D5, Novocastra Lab. Ltd., UK) at a dilution

of 1:50 in PBS.

Briefly rinsed in PBS, sections, which were incubated with desmin, plectin or α-actinin antibody, were then reacted with Alexa Fluor™ 488 goat anti-mouse IgG conjugate (Molecular Probes, Eugene, OR) at a dilution of 1:100 in PBS for 2 hr at room temperature. They were coverslipped with 90% nonfluorescent glycerol containing 2 mg/ml 1,4-diazabicyclo [2,2,2] octane (DABCO) and 7.5 µg/ml 4,6-diamino-2-phenylindole dihydrochloride (DAPI) in PBS, and examined in a Carl Zeiss LSM 410 confocal laser scanning microscope.

Sections, which were incubated with ß dystroglycan antibody, were then treated by the indirect immunoperoxidase method, using a Histofine Simple Stain PO Kit (Nichirei, Tokyo, Japan). The peroxidase complex was visualized by treatment with a freshly prepared solution of 0.1 mg/ml diaminobenzidine tetrahydrochloride (DAB) and 0.01% H_2O_2 for 7 min at room temperature.

Specificity of the above immunoreactivities was confirmed by replacing the primary antibody for normal rabbit serum or PBS. Specificity of mouse anti-desmin mAb (Yamanouchi et al., 2000), mouse anti-plectin mAb (Hijikata et al., 1999), mouse anti-α-actinin mAb (Flick and Konieczny, 2000), and mouse anti-ß dystroglycan mAb (Ueda et al., 1998) has already been demonstrated.

As ß dystroglycan, which is a component of the sarcolemmal proteins, exhibited a high immunoreactive contrast of the sarcolemma, ß dystroglycan-immunoreacted sections were utilized for measurements of the cross-sectional area (CSA) per fifty randomly-selected muscle fibers from all groups, using an image analysis device (Nikon Cosmosome, IS, Tokyo, Japan).

Double immunofluorescence labeling

Sections which were mounted on slide glasses were treated with 10% normal goat serum for 20 min at room temperature. They were then incubated either with rabbit anti-desmin polyclonal antibody (pAb, Sigma Chemical Co., St. Louis, MO) at a dilution of 1:20 in PBS and mouse anti-plectin mAb at a dilution of 1:100 in PBS, or with rabbit anti-desmin pAb at a dilution of 1:20 in PBS and mouse anti-α-actinin mAb at a dilution of 1:400 in PBS, respectively. After being briefly rinsed with PBS, sections were reacted with Alexa Fluor™ 594 goat anti-rabbit IgG conjugate (for desmin), or with Alexa Fluor™ 488 goat anti-mouse IgG conjugate (for plectin and α-actinin) at a dilution of 1:100 in PBS for 2 hr at room temperature. After the above mentioned coverslipping procedures, they were examined in the confocal laser scanning microscope.

Specificity for the above double immuno-fluorescence labelings was confirmed by replacing rabbit anti-desmin pAb and/or mouse anti-plectin mAb for PBS, and by replacing rabbit anti-desmin pAb and/or mouse anti-α-actinin mAb for PBS. Specificity of rabbit anti-desmin pAb has already been demonstrated by Reipert et al. (1999).

Statistical analysis

Values of blood serum assays and CSA from all groups were examined for significance by the t-test and ANOVA. All data were expressed as mean ± SEM.

Results

CSA of the CG, HSG and RG

We utilized ß dystroglycan-immunoreacted sections for measurements of the CSA among the CG, HSG and RG, and we found no significant differences in the sarcolemmal immunoreactive intensity among these groups (Fig. 1). The reduction of the CSA significantly occurred in the HSG from the first week and became more pronounced at 4 weeks, when compared to that of the CG (Fig. 2). As indicated by this figure, the CSA of the RG was not completely recovered at 2 weeks, when compared to that of the CG.

Ultrastructural alteration of the HSG and RG

As previously described by others, waving and distortion of Z-disc alignment, generally called Z-streaming of myofibrils, uniquely occurred in the HSG from the first week (Fig. 3a). However, Z-streaming was

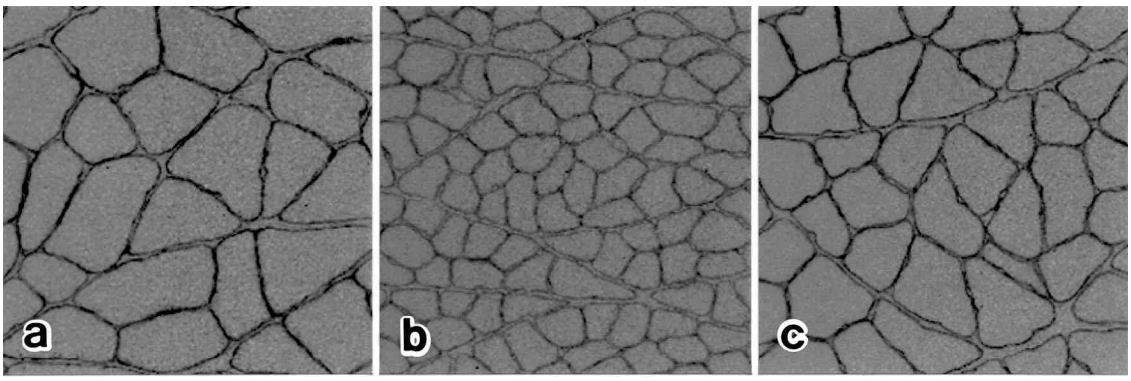

Fig. 1. Immunoreactivity for ß dystroglycan of soleus muscle fibers in CG **(a)**, HSG **(b)** and RG **(c)**. Muscle atrophy remarkably occurs in HSG at 4 weeks **(b)** in comparison with CG at 4 weeks **(a)**, and a complete recovery of CSA does not occur in RG at 2 weeks **(c)**. x 150

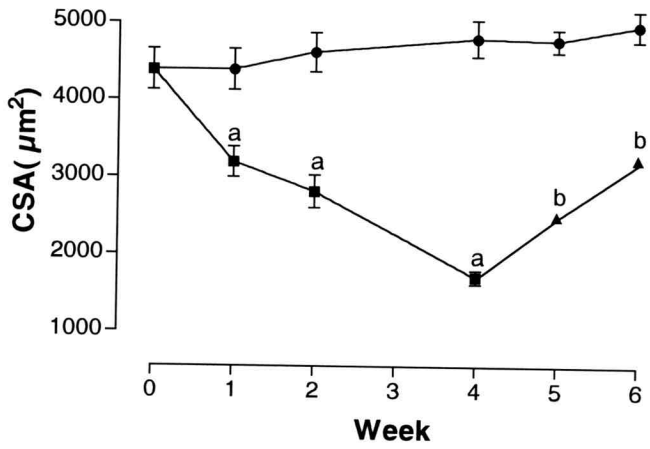

seldom encountered in the RG at 2 weeks (Fig. 3b).

Immunoreactivity for desmin, plectin and α-actinin of the CG

Immunoreactivities for desmin and plectin in soleus muscle fibers of the CG were preferentially localized along the sarcolemma as well as in the sarcoplasm (Fig. 4a,b). As shown in these figures, both desmin and plectin exhibited honey-comb immunoreactive patterns

Fig. 2. Comparison of cross-sectional areas (CSA) of soleus muscle fibers among CG (circle), HSG (square) and RG (triangle), using ß dystroglycan-immunoreacted sections. Bars represent mean ± SEM. a: $p<0.01$ (compared with value of HSG before hindlimb suspension). b: $p<0.01$ (compared with value of HSG at 4 weeks).

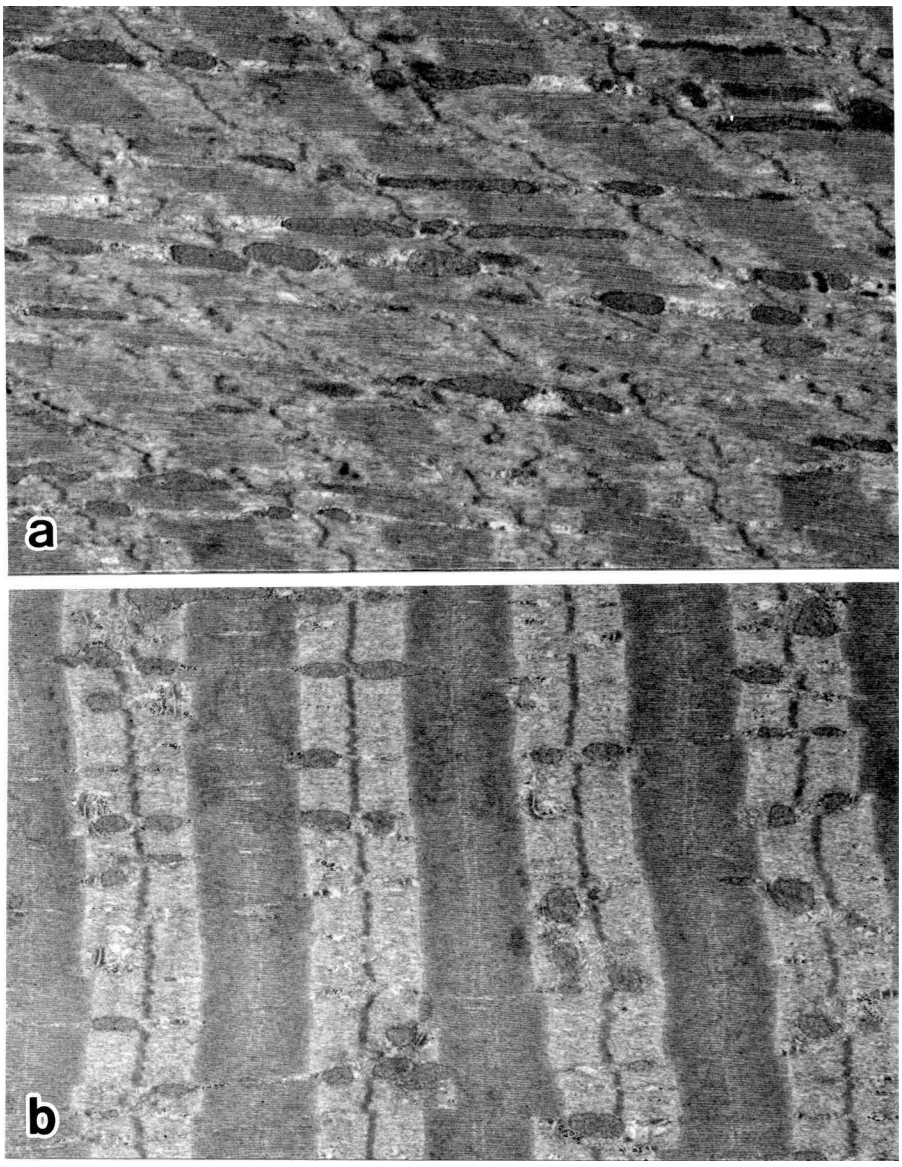

Fig. 3. Electron micrographs showing Z-streaming of soleus muscle fiber in HSG at 2 weeks **(a)** and its restoration in RG at 2 weeks **(b)**. x 12,000

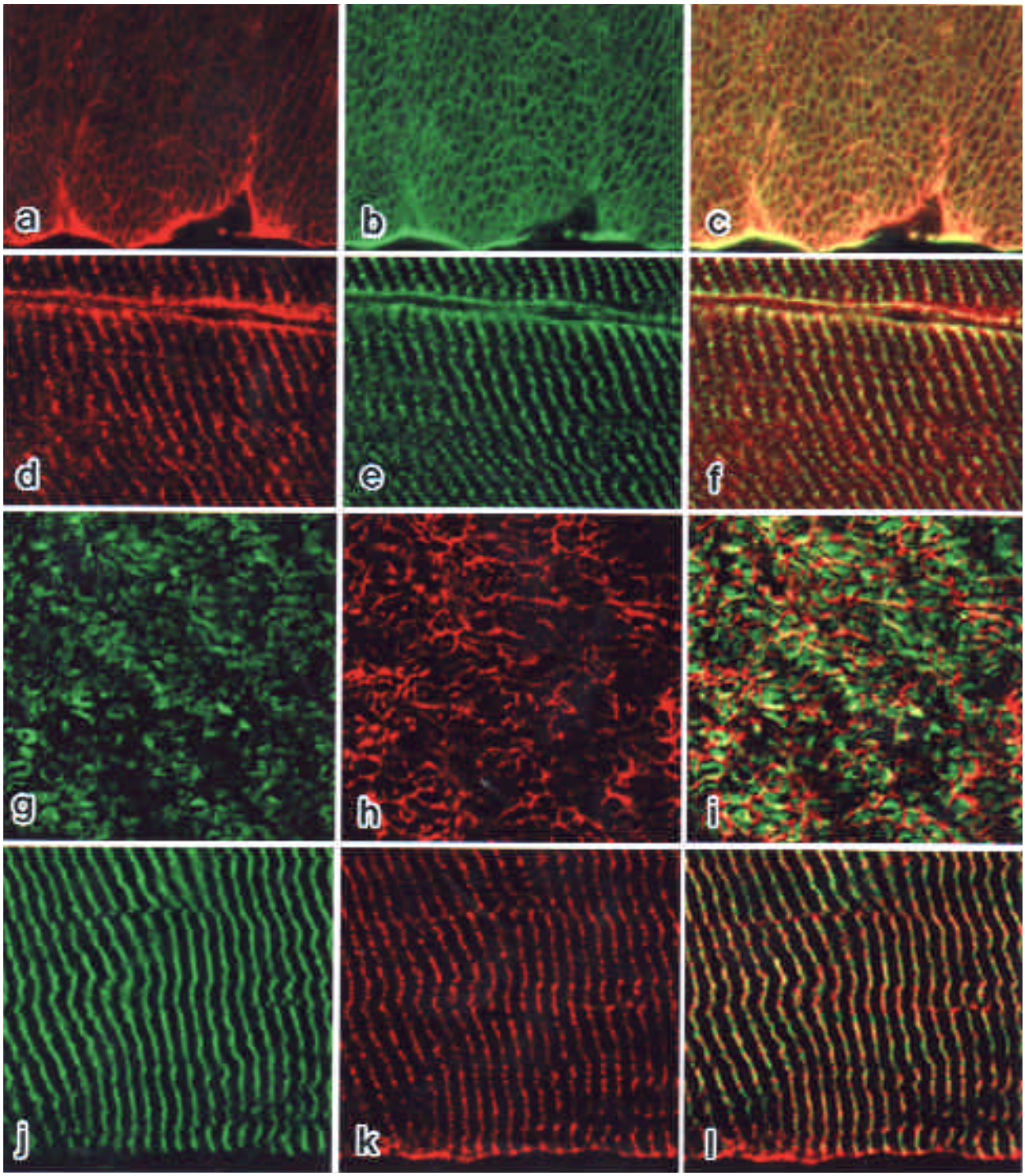

Fig. 4. a-c. Immunoreactivities for desmin (red signals in **a**), plectin (green signals in **b**), and almost complete overlapped superimposed images of desmin and plectin immunoreactivities (yellow signals in **c**) in a single cross-section of sarcoplasm in CG at 4 weeks. **d-f**. Immunoreactivities for desmin (red signals in **d**), plectin (green signals in **e**), and almost complete overlapped superimposed images of desmin and plectin immunoreactivities (yellow signals in **f**) in a single longitudinal section of sarcoplasm in CG at 4 weeks. **g-i.** Immunoreactivities for α-actinin (green signals in **g**), desmin (red signals in **h**), and a few overlapped superimposed images of α-actinin and desmin immunoreactivities in a single cross-section of CG at 4 weeks. **j-l**. Immunoreactivities for α-actinin (green signals in **j**), desmin (red signals in **k**), and discontinuous overlapped superimposed images of α-actinin and desmin immunoreactivities (yellow signals in **l**) in a single longitudinal section of CG at 4 weeks. a-f, x 1,300; g-l, x 1,500

extending throughout the sarcoplasm in the cross-sections. By double immunofluorescence labeling of desmin (red signals in Fig. 4a) and plectin (green signals in Fig. 4b) in a single cross-section, superimposed images of honey-comb patterns of desmin and plectin were almost completely overlapped (yellow signals in Fig. 4c). In a longitudinal section, immunoreactivity for both signals exhibited bands with a regular periodicity (Fig. 4d,e), and superimposed images of both immunoreactivities exhibited almost complete overlapping (yellow signals in Fig. 4f).

Figure 4g,h show immunoreactivities for α-actinin (green signals in Fig. 4g) and desmin (red signals in Fig. 4h) in a single cross-section, and Figures 4j and 4k show both immunoreactivities in a single longitudinal section, respectively. In superimposed images, a considerable number of green and red signals remained in the cross-section (Fig. 4i). On the contrary, both signals were discontinuously overlapped (yellow signals in Fig. 4l) at the level of Z-discs in the longitudinal section.

Disorganization of honey-comb immunoreactive pattern of desmin and plectin in the HSG

Fig. 5a,c show honey-comb immunoreactive patterns of desmin and plectin in the sarcoplasm of cross-sectioned soleus muscle fibers of the CG, respectively. The disorganization of both immunoreactive patterns occurred in the sarcoplasmic areas of most atrophic muscle fibers of the HSG from the first week (Fig. 5b,d). The appearance of the disorganized honey-comb pattern greatly varied from muscle fiber to fiber as well as from sarcoplasmic area to area (Fig. 5b,d). Although such disorganized areas increased in degree in proportion to the suspension period, we encountered muscle fibers which almost completely retained the honey-comb pattern throughout the experiment.

As already demonstrated by Fig. 4g, immunoreactivity for α-actinin exhibited a ripple-like pattern running almost parallel throughout the sarcoplasm in a cross-section (Fig. 5e). However, the disorganization of such a structure occurred in most of the HSG from the first week, and increased in degree with the appearance of aggregates of linear-like immunoreactivities almost in the center of atrophic muscle fibers of the HSG from 2 weeks (Fig. 5f).

Recovery of honey-comb immunoreactive pattern of desmin and plectin in the RG

The disorganization of honey-comb immunoreactive patterns in the HSG, as shown in Fig. 5b,d, remarkably decreased in the RG from the first week, occasionally showing the central nuclei, as described in the recovery process of atrophic muscle fibers by many researchers. Such honey-comb patterns of desmin and plectin were almost completely restored in most muscle fibers of the RG at 2 weeks, when compared to those of the CG at 6 weeks (Fig. 6a,b).

Evaluation of disorganization and restoration of honey-comb immunoreactive pattern

For evaluation of the disorganization and restoration of honey-comb immunoreactive patterns throughout the experiment, we examined the appearance frequency of muscle fibers in which sarcoplasmic areas showing disorganized honey-comb patterns occupied more than 10% of the total sarcoplasmic areas in the laser scanning microscope, using an NIH image analysis software, and the frequency per 100 muscle fibers each was compared among the CG, HSG and RG, respectively (Table 2). As represented in this table, the frequency of muscle fibers occupying more than 10% of the disorganized areas increased from 2 weeks in the HSG, although such muscle fibers were not encountered in the CG throughout the experiment. Muscle fibers occupying more than 10% of the disorganized areas were rarely

Table 1. Total protein, albumin and total cholesterol values in blood serum of the CG, HSG and RG.

GROUP	TOTAL PROTEIN (g/dl)	ALBUMIN (g/dl)	TOTAL CHOLESTEROL (mg/dl)
CG			
1 week (n=6)	5.41±0.12	4.06±0.07	50.00±3.16
2 weeks (n=6)	5.61±0.08	4.28±0.11	55.33±6.43
4 weeks (n=6)	5.51±0.16	3.90±0.13	57.50±3.78
5 weeks (n=6)	5.47±0.17	3.90±0.14	50.50±7.96
6 weeks (n=6)	5.78±0.12	4.14±0.08	59.00±7.34
HSG			
1 week (n=6)	5.05±0.14	3.53±0.11[a]	53.50±5.69
2 weeks (n=7)	5.37±0.09	3.68±0.13[b]	55.29±2.83
4 weeks (n=7)	5.25±0.10	3.70±0.09	56.00±4.02
RG			
1 week (n=6)	5.43±0.16	3.68±0.14	55.00±4.74
2 weeks (n=6)	5.56±0.16	3.98±0.14	54.17±5.10

Values are expressed by mean±SEM. [a]: $p<0.05$ (comparison between the CG and HSG at 1 week). [b]: $p<0.01$ (comparison between the CG and HSG at 2 weeks).

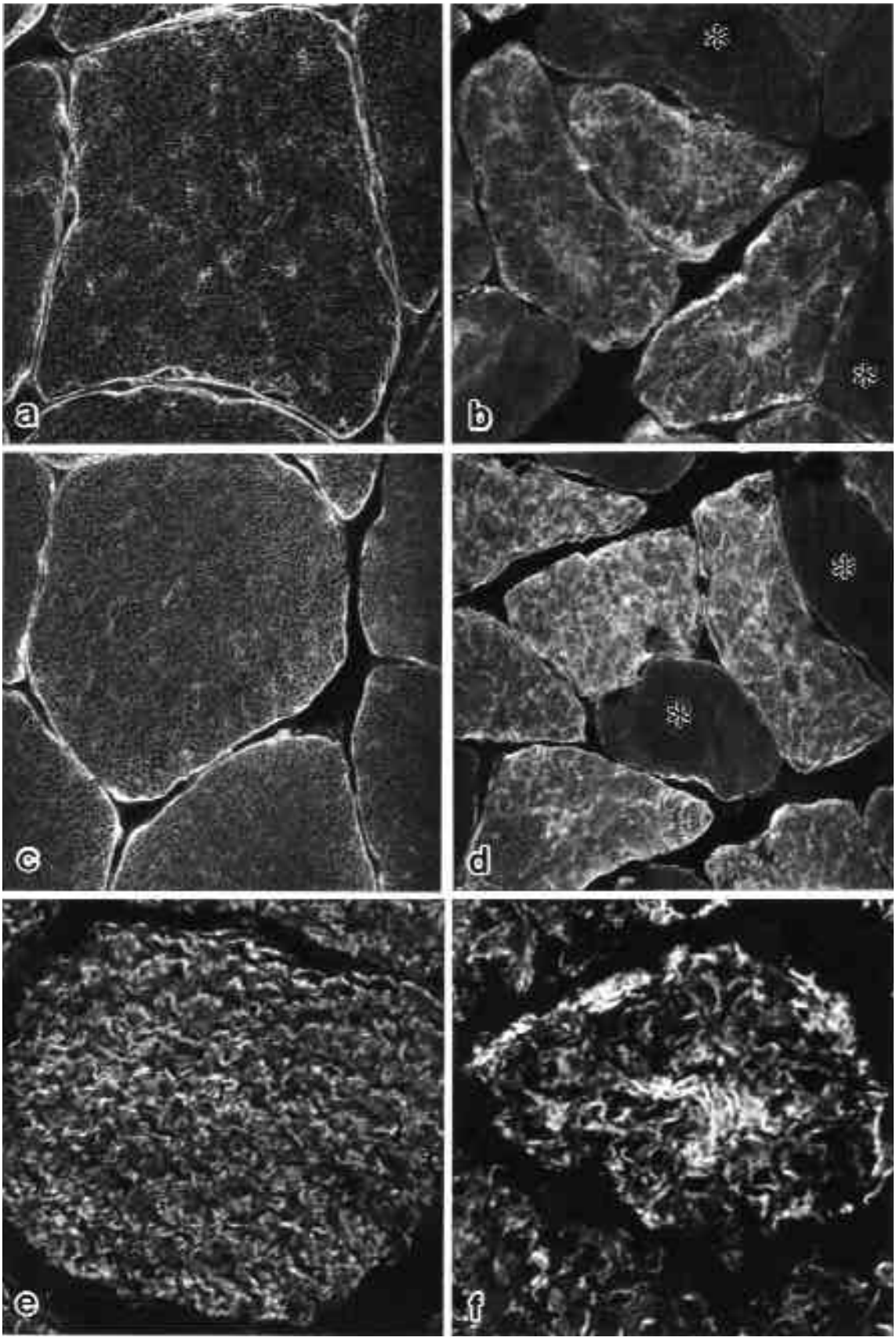

Fig. 5.
Disorganization of immunoreactive patterns of desmin, plectin and α-actinin in sarcoplasm of HSG. **a.** Honey-comb pattern of desmin in sarcoplasm of muscle fibers in CG at 2 weeks. **b.** Disorganized honey-comb pattern of desmin in HSG at 2 weeks. Some muscle fibers (asterisks) still retain honey-comb pattern. **c.** Honey-comb pattern of plectin in CG at 2 weeks. **d.** Disorganized honey-comb pattern of plectin in HSG at 2 weeks. Honey-comb pattern still remains in some muscle fibers (asterisks). **e.** Immunoreactivity for α-actinin showing a rather parallel-arranged ripple-like structure in CG at 2 weeks. **f.** Disorganization of ripple-like structure, associated with immunoreactive aggregates almost in the center of sarcoplasm in HSG at 2 weeks. a-d, x 600; e, x 1,200; f, x 1,500

encountered in the RG at 2 weeks.

Discussion

In the present study of the rat atrophic soleus muscle induced by hindlimb suspension, we utilized male Wistar rats aged 12 weeks only, as these animals are considered to complete a rapid growth and maintain an almost constant proportion of fiber types in their soleus muscles at this age, according to the physiological data by Okada et al. (1981). In the blood serum assays of the HSG, only albumin values showed a slight fall by 2 weeks but were recovered within normal levels at 4 weeks, when compared to those of the CG (Table 1). Thus, we decided to utilize these animals as atrophic soleus muscle models although the effects of malnutrition on muscle atrophy could not completely be ruled out in the HSG by 2 weeks. Soleus muscle atrophy of the HSG was confirmed by the decrease of CSA in the HSG, when compared to those of the CG, as shown in Figure 2.

By ultrastructural and immunocytochemical analyses of the rat diaphragma, Hijikata et al. (1999) proposed three-dimensional topological and structural relationships of both desmin and plectin with Z-discs, manifested by immunoreactivity for α-actinin. These researchers explained that plectin links desmin threads to Z-discs and connect the adjacent desmin threads to each other. They also suggested that the formation of lateral linkages among adjacent Z-discs by desmin and plectin may be structural components, which are indispensable for normal synchronized and harmonized contraction and relaxation in effective force generation of muscle fibers. Using immunoelectron microscopy, Schröder et al. (1999) also confirmed the topological relationship between plectin and Z-discs in human skeletal muscle fibers.

In our analyses of location of desmin, plectin and α-actinin in rat soleus muscle fibers using double immunofluorescence labeling, as demonstrated in Figure 4, we found no fundamental inconsistencies in the location of these components with the previous reports. Honey-comb immunoreactive patterns extending throughout the sarcoplasm were almost completely overlapped by double immunofluorescence labeling as revealed by cross-sectioned profiles. Therefore, we consider, at present, that desmin and plectin are in a close apposition to each other, and both components surrounding myofibrils are involved in the connection with Z-discs.

Table 2. Evaluation of disorganization and reorganization of honey-comb immunoreactive pattern of desmin and plectin among the CG, HSG and RG.

GROUP	DESMIN (number/100 muscle fibers)	PLECTIN (number/100 muscle fibers)
CG		
1 week (n=6)	-	-
2 weeks (n=6)	-	-
4 weeks (n=6)	-	-
5 weeks (n=4)	-	-
6 weeks (n=5)	-	-
HSG		
1 week (n=6)	-	-
2 weeks (n=7)	4.33±3.15	16.37±7.95
4 weeks (n=7)	21.41±4.32	27.28±3.26
RG		
1 week (n=6)	0.87±0.39	0.50±0.31
2 weeks (n=6)	0.41±0.80	0.76±0.21

Values indicate appearance frequency of muscle fibers occupying more than 10% of disorganized sarcoplasmic area per total sarcoplasmic area among 100 muscle fibers each, expressed by mean±SEM.

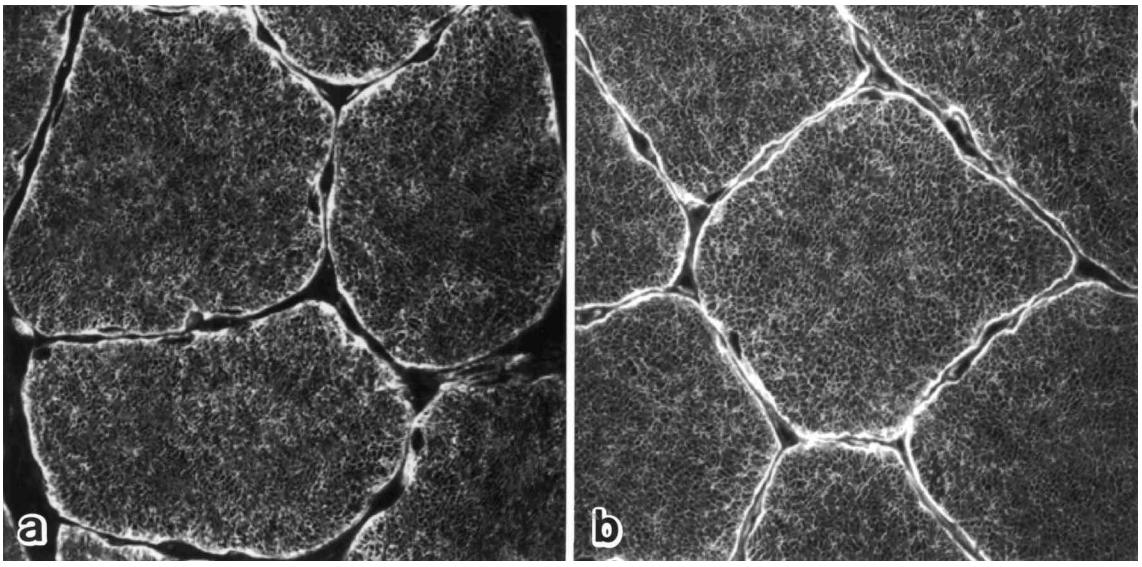

Fig. 6. Restoration of honey-comb immunoreactive patterns of desmin **(a)** and plectin **(b)** in sarcoplasm of muscle fibers in RG at 2 weeks. x 1,000

Our immunocytochemical analyses revealed the onset of disorganization of honey-comb immunoreactive patterns of desmin and plectin in the HSG from the first week. Such disorganized patterns gradually increased in degree in proportion to the suspension period, as shown in Table 2. Since Schröder et al. (2000) insisted on the role of desmin and plectin in the intermyofibrillar scaffold, we consider, at present, that the disorganization in topological and structural relationships of desmin and plectin with Z-discs surrounding myofibrils, which is primarily induced in atrophic muscle fibers by hindlimb suspension, lead to Z-streaming.

The disorganization greatly varied from muscle fiber to fiber in the HSG. Soleus muscle fibers, which did not show any disorganization of honey-comb pattern, existed in the HSG throughout the experiment. Thus, further analyses are necessary to elucidate whether such a diversity among soleus muscle fibers depends on the difference in fiber types, using specific myosin antibodies.

The recovery of atrophic muscles after removal of restricted muscle movement was investigated by Lieber et al. (1989) and Mozdziak et al. (2000). These researchers stated that the recovery of the CSA as well as the diameter of muscle fibers was not completed even at 4 weeks. Also, in our samples of the RG, a full recovery of the CSA was not established at 2 weeks. However, our immunocytochemical study indicated that the disorganization of honey-comb patterns of desmin and plectin as well as the disorganization of α-actinin were almost completely restored in most of the sarcoplasm at 2 weeks in the RG, allowing muscle movement by unrestricted cage activity. This restoration was inevitably followed by the disappearance of Z-streaming. How such an early recovery in arrangement of desmin and plectin relating with Z-discs occurs and whether new synthesis of these components is required for the re-arrangement remain uncertain.

In conclusion, rat hindlimb suspension evoked the disorganization of honey-comb patterns of desmin and plectin connected with Z-discs in atrophic soleus muscle fibers which lead to Z-streaming, and removal of the restricted muscle movement induced the restoration of the reorganization of the honey-comb pattern prior to the recovery of the CSA.

Acknowledgements. Dr. Soichiro Nara expresses thanks to emeritus Prof. Harunori Ishikawa, Gunma University, for his valuable advice for this work. The authors thank Ms. Toyono Nobukuni for her secretarial help.

References

Andrä K., Lassmann H., Bittner R., Shorny S., Fassler R., Propst F. and Wiche G. (1997). Targeted inactivation of plectin reveals essential function in maintaining the integrity of skin, muscle, and heart cytoarchitecture. Genes Dev. 11, 3143-3156.

Bennett G.S., Fellini S.A., Toyama Y. and Holtzer H. (1979). Redistribution of intermediate filament subunits during skeletal myogenesis and maturation in vitro. J. Cell Biol. 82, 577-584.

Booth F.W. (1977). Time course of muscular atrophy during immobilization of hindlimbs in rats. J. Appl. Physiol. 43, 656-661.

Booth F.W. and Gollnick P.D. (1983). Effects of disuse on the structure and function of skeletal muscle. Med. Sci. Sports Exerc. 15, 415-420.

Brooks S.E. (1995). Ultrastructure of voluntary muscle in childhood malnutrition. West Indian Med. J. 44, 133-139.

Cooper R.R. (1972). Alterations during immobilization and regeneration of skeletal muscle in cats. J. Bone Joint Surg. Am. 54, 919-953.

Desplanches D., Mayet M.H., Sempore B. and Flandrois R. (1987). Structural and functional responses to prolonged hindlimb suspension in rat muscle. J. Appl. Physiol. 63, 568-583.

Fitts R.H. and Brimmer C.J. (1985). Recovery in skeletal muscle contractile function after prolonged hindlimb immobilization. J. Appl. Physiol. 59, 916-923.

Fitts R.H., Metzger J.M., Riley D.A. and Unsworth B.R. (1986). Models of disuse: a comparison of hindlimb suspension and immobilization. J. Appl. Physiol. 60, 1946-1953.

Fitts R.H., Riley D.R. and Widrick J.J. (2000). Physiology of a microgravity environment invited review: microgravity and skeletal muscle. J. Appl. Physiol. 89, 823-839.

Flick M.J. and Konieczny S.F. (2000). The muscle regulatory and structural protein MLP is a cytoskeletal binding partner of ßI-spectrin. J. Cell Sci. 113, 1553-1564.

Foisner R. and Wiche G. (1991). Intermediate filament-associated proteins. Curr. Opin. Cell Biol. 3, 75-81.

Gache Y., Chavanas S., Lacour J.P., Wiche G., Owaribe K., Meneguzzi G. and Ortonne J.P. (1996). Defective expression of plectin/HD1 in epidermolysis bullosa simplex with muscular dystrophy. J. Clin. Invest. 15, 2289-2298.

Goldspink D.F. (1977). The influence of immobilization and stretch on protein turnover of rat skeletal muscle. J. Physiol. 264, 267-282.

Hansen-Smith F.M., Picou D. and Golden M.H. (1979). Growth of muscle fibres during recovery from severe malnutrition in Jamaican infants. Br. J. Nutr. 41, 275-282.

Hauschka E.O., Roy R.R. and Edgerton V.R. (1988). Periodic weight support effects on rat soleus fibers after hindlimb suspension. J. Appl. Physiol. 65, 1231-1237.

Hijikata T., Murakami T., Imamura M., Fujimaki N. and Ishikawa H. (1999). Plectin is a linker of intermediate filaments to Z-discs in skeletal muscle fibers. J. Cell Sci. 112, 867-876.

Ishikawa H., Bischoff R. and Holtzer H. (1968). Mitosis and intermediate-sized filaments in developing skeletal muscle. J. Cell Biol. 38, 538-555.

Lazarides E. (1980). Intermediate filaments as mechanical integrators of cellular space. Nature 283, 249-256.

Li Z., Colucci-Guyon E., Pincon-Raymond M., Mericskay M., Pournin S., Paulin D. and Babinet C. (1996). Cardiovascular lesions and skeletal myopathy in mice lacking desmin. Dev. Biol. 175, 362-366.

Lieber R.L., McKee-Woodburn T. and Gershuni D.H. (1989). Recovery of the dog quadriceps after 10 weeks of immobilization followed by 4 weeks of remobilization. J. Orthop. Res. 7, 408-412.

Lippmann R.K. and Selig S. (1928). An experimental study of muscle atrophy. Surg. Gynecol. Obstet. 47, 512-522.

Milner D.J., Weitzer G., Tran D., Bradley A. and Capetanaki Y. (1996). Disruption of muscle architecture and myocardial degeneration in mice lacking desmin. J. Cell Biol. 134, 1255-1270.

Mozdziak P.E., Pulvermacher P.M. and Schultz E. (2000). Unloading of juvenile muscle results in a reduced muscle size 9 wk after reloading. J. Appl. Physiol. 88, 158-164.

Okada S., Nonaka I., Ishimura S. and Sugita H. (1981). A histochemical study of muscle fiber differentiation in the rat muscle. Shinkeinaika 15, 363-370.

Price D.L., Cork L.C., Struble R.G., Kitt C.A., Walker L.C., Powers R.E., Whitehouse P.J. and Griffin J.W. (1987). Dysfunction and death of neurons in human degenerative neurological diseases and in animal models. Ciba Found. Symp. 126, 30-48.

Reipert S., Steinböck F., Fischer I., Bittner R.E., Zeöld A. and Wiche G. (1999). Association of mitochondria with plectin and desmin intermediate filaments in striated muscle. Exp. Cell Res. 252, 479-491.

Russman B.S., Melchreit R. and Drennan J.C. (1983). Spinal muscular atrophy: the natural course of disease. Muscle Nerve 6, 179-181.

Schröder R., Mundegar R.R., Treusch M., Schlegel U., Blümcke I., Owaribe K. and Magin T.M. (1997). Altered distribution of plectin/HD1 in dystrophinopathies. Eur. J. Cell Biol. 74, 165-171.

Schröder R., Warlo I., Herrmann H., van der Ven P.F.M., Klasen C., Blümcke I., Mundegar R.R., Fürst D.O., Goebel H.H. and Magin T.M. (1999). Immunogold EM reveals a close association of plectin and the desmin cytoskeleton in human skeletal muscle. Eur. J. Cell Biol. 78, 288-295.

Schröder R., Fürst D.O., Klasen C., Reimann J., Herrmann H. and van der Ven P.F.M. (2000). Association of plectin with Z-discs is a prerequisite for the formation of the intermyofibrillar desmin cytoskeleton. Lab. Invest. 80, 455-464.

Thomason D.B., Herrick R.E., Surdyka D. and Baldwin K.M. (1987). Time course of soleus muscle myosin expression during hindlimb suspension and recovery. J. Appl. Physiol. 63, 130-137.

Thompsen P. and Luco J.V. (1944). Changes of weight and neuromuscular transmission in muscles of immobilized joints. J. Neurophysiol. 7, 246-251.

Tomanek R.J. and Lund D.D. (1974). Degeneration of different types of skeletal muscle fibres. II. Immobilization. J. Anat. 118, 531-541.

Ueda H., Gohdo T. and Ohno S. (1998). ß-Dystroglycan localization in the photoreceptor and Müller cells in the rat retina revealed by immunoelectron microscopy. J. Histochem. Cytochem. 46, 185-191.

Valtat E. (1877). De l'atrophie musculaire consecutive aux maladies des articulations. Gerner-Balliére, Paris

van Balkom R.H., van der Heijden H.F., van Herwaarden C.L. and Dekhuijzen P.N. (1994). Corticosteroid-induced myopathy of the respiratory muscles. Neth. J. Med. 45, 114-122.

Wiche G., Krepler R., Artlieb U., Pytela R. and Denk H. (1983). Occurrence and immunolocalization of plectin in tissues. J. Cell Biol. 97, 887-901.

Witzmann F.A., Kim D.H. and Fitts R.H. (1982). Hindlimb immobilization: length-tension and contractile properties of skeletal muscle. J. Appl. Physiol. 53, 335-345.

Yamanouchi K., Soeta C., Naito K. and Tojo H. (2000). Expression of myostatin gene in regenerating skeletal muscle of the rat and its localization. Biochem. Biophys. Res. Commun. 270, 510-516.

Zurcher R.M., Horber F.F., Grunig B.E. and Frey F.J. (1989). Effect of thyroid dysfunction on thigh muscle efficiency. J. Clin. Endocrinol. Metab. 69, 1082-1086.

Accepted December 24, 2001